Evolution of the magnetic field–temperature phase diagram in $UAs_{1-x}Se_x$

Tomasz Plackowski, Marcin Matusiak, and Jozef Sznajd
Institute of Low Temperature and Structural Research, Polish Academy of Sciences, P.O. Box 1410, 50-950 Wroclaw, Poland
(Received 10 May 2010; revised manuscript received 21 July 2010; published 3 September 2010)

The evolution of the magnetic field–temperature phase diagram of $UAs_{1-x}Se_x$ with x in the range of 0–0.1 is studied by means of magnetocaloric and specific-heat measurements. Our interest is focused on the high-temperature phase transitions and especially on the point, where the paramagnetic (P) and two ordered phases meet. For undoped UAs these two ordered states are the ferrimagnetic (Fi) and the type-I antiferromagnetic phases. According to Sinha *et al.* [Phys. Rev. Lett. **45**, 1028 (1980)] the antiferromagnetic phase transition is in the vicinity of a Lifshitz point. Furthermore, Kuznietz *et al.* [J. Magn. Magn. Mater. **61**, 246 (1986)] showed that an incommensurate phase (IC) emerges between the type-I (or type-IA) antiferromagnetic and paramagnetic phases in the case of $UAs_{1-x}Se_x$ with $0<x<0.15$ in zero magnetic field. The results reported in this paper show the existence of a $T_{Fi/IC}(B)$ line that separates the ferrimagnetic region from a phase, which cannot be identified on the basis of our thermodynamic measurements. However, one may assume it is the IC phase, consistent with the above mentioned zero field results. The $T_{Fi/IC}(B)$ line merges with the order-disorder line at point (B_p, T_p), where the critical line (IC/P) meets with two first order transitions lines: Fi/P and Fi/IC. This point can be considered as an analog of a Lifshitz point. A simple phenomenological description of the phase transitions near this special point is provided.

DOI: 10.1103/PhysRevB.82.094408 PACS number(s): 71.27.+a, 05.10.Cc

I. INTRODUCTION

The magnetic phase diagram of $UAs_{1-x}Se_x$ solid solutions has been the subject of extensive investigations for more than 40 years. In spite of this, the complex magnetic properties of such a system are still far from being fully understood. The first studies of the x-T magnetic phase diagram of this system were reported by Obolenski and Troc on the polycrystalline samples.[1] These were followed by results obtained on single-crystalline samples by Vogt and Bartholin.[2] The latter work was also the first attempt to investigate the U(As,Se) system in an applied magnetic field of up to 18 T. The authors of Ref. 2 presented a set of B-T diagrams that turned out to be very complex. In undoped UAs a sufficiently high magnetic field applied along [001] direction induces high- and low-temperature ferrimagnetic phases in addition to the zero-field type-I (AI) and type-IA (AIA) antiferromagnetic phases. Both of the high temperature phase transitions, i.e., the disordered to type-I for $B<B_p$ and disordered to ferrimagnetic for $B>B_p$ (where B_p and T_p are the coordinates of the triple point), are of first order. The magnetic behavior of pure UAs is altered by selenium substitution. In $UAs_{1-x}Se_x$ (up to $x=0.6$) a modulated magnetic structure emerges below the transition to the paramagnetic state (P) at T_N. This structure has been identified by means of very detailed neutron diffraction measurements to be an incommensurate phase (IC).[3–5] More recently x-ray magnetic scattering studies added several important details, including the discovery of a new magnetic phase, to the phase diagram of $UAs_{1-x}Se_x$.[6,7] Subsequent measurements of resonant x-ray scattering at the U M_4 edge allowed further investigation of the multi-k magnetic structures in $UAs_{0.8}Se_{0.2}$.[8,9]

In this paper, we focus mainly on the high-temperature phase transition from the paramagnetic to the ordered states in single-crystalline $UAs_{1-x}Se_x$ with $x \leq 0.1$. In UAs both high temperature phases are collinear single **k** structures composed of a stack of ferromagnetic planes (001). In the low-field AI phase the spins in the neighboring planes are alternatively directed up and down (+−+−) along the ⟨001⟩ axis. The spins of the ferromagnetic planes are ordered in the (++−) sequence in the high field ferrimagnetic phase. What concerns the paramagnetic-antiferromagnetic phase transition, neutron experiments suggested that UAs will order into an incommensurate state. A weakly first-order phase transition occurs to the type-I antiferromagnetic state takes place instead.[10,11] Consequently, the authors of Ref. 10 conclude that the AI/P transition is in a vicinity of a Lifshitz point (LP). As shown in Ref. 2, doping of UAs with Se stabilizes the incommensurate phase characterized by a wave vector $\mathbf{k}=[00k]$. The exact form of this phase is not determined. However at $B=0$ two scenarios are possible depending on the doping ratio: (i) a sequence of IC-AI-AIA transitions or (ii) IC phase transforms directly to the type-IA antiferromagnetic (++−−) phase. Thus, one of the aims of our investigations is to check experimentally if a multicritical point in which paramagnetic, commensurate, and incommensurate phases meet is attainable in $UAs_{1-x}Se_x$ and if this is the tricritical Lifshitz point.

II. EXPERIMENTAL

Single crystals of $UAs_{1-x}Se_x$ were grown at ETH Zurich, Switzerland by a technique called mineralization. A pressed pellet with the desired composition was kept at about 50 C below the melting temperature for several weeks. The procedure is described in detail elsewhere.[12] The isothermal magnetocaloric coefficient (M_T) and specific heat (C_B) data were obtained using a heat-flow calorimeter.[13] In this method the sample is connected to a heat sink by means of a sensitive heat-flow meter of high thermal conductance. $C_B(T)$ curves are collected while sweeping the temperature at a constant magnetic field, whereas $M_T(B)$ during field sweeps at a con-

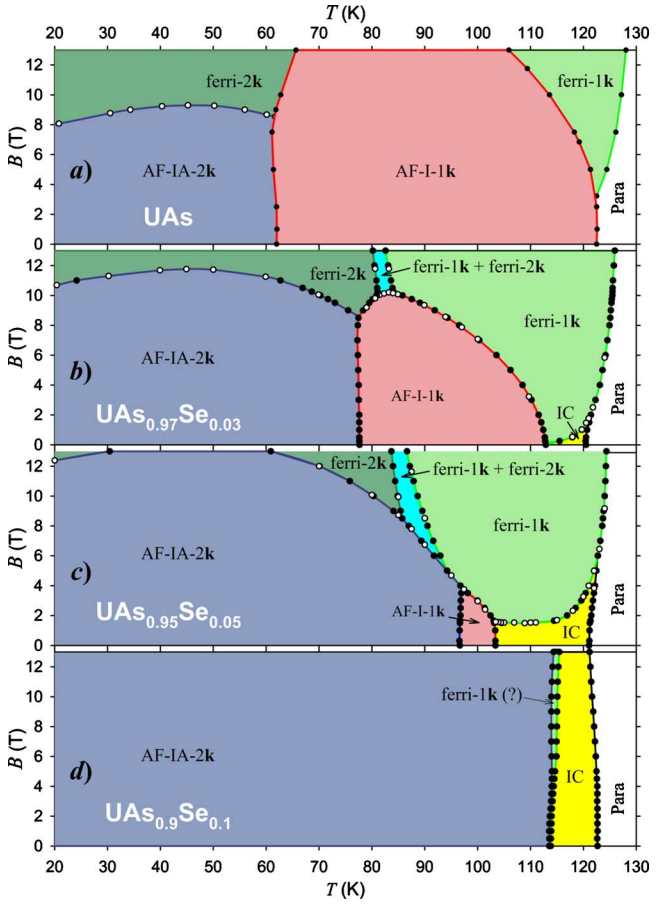

FIG. 1. (Color online) The evolution of the B-T phase diagram of $UAs_{1-x}Se_x$. Data points were obtained from specific heat (solid points) and magnetocaloric (open points) measurements.

stant temperature. Single crystals of $UAs_{1-x}Se_x$ were glued to the heat-flow meter using Collaprene (Gubra, Milan, Italy) with the ⟨001⟩ axis oriented parallel to the magnetic field. A sample was surrounded by a double passive radiation screen (gold plated), and both screens were in a good thermal contact with the sink. The whole ensemble was evacuated down to 10^{-6} hPa and placed in the gas-flow variable-temperature insert of the Oxford Instruments cryostat fitted with a 13/15 T superconducting magnet. Temperature dependences of the magnetization and magnetic susceptibility in a magnetic field up to 9 T were measured using a Quantum Design Physical Property Measurement System (PPMS).

III. RESULTS

Figure 1 shows the doping evolution of the B-T phase diagram of $UAs_{1-x}Se_x$ with the magnetic field is applied along the ⟨001⟩ crystallographic axis. We studied four single crystals with $x=0$ (undoped), 0.03. 0.05, and 0.1 selenium content. The diagrams were constructed by combining magnetocaloric and specific-heat measurements. Analogous B-T diagrams for single-crystalline samples with $x=0.025$, 0.05, 0.25, 0.30, and 0.40, were presented by Vogt and Bartholin.[2] All of the results obtained there were based on magnetic measurements. The authors of Ref. 2 mentioned for the first time the existence of a modulated structure preceding the transition to the paramagnetic state[2] but they were unable to detect the exact position of the Fi-1**k**/IC transition line for $x \leq 0.05$. This $T_{\mathrm{Fi/IC}}(B)$ line is clearly visible in our thermodynamic results (Fig. 1, panels b and c). It is worth noting that the horizontal-like transition lines on the investigated B-T diagrams could not be properly detected with the aid of $C_B(T)$ dependences because specific-heat anomalies in such cases are smeared over a wide temperature range. Therefore, measurements of the magnetocaloric coefficient were truly irreplaceable. The different types of magnetic order in the distinct magnetic phases were identified according to the results of neutron-diffraction studies available in literature.[5,14,15] Our results do not provide a clear evidence of the incommensurate phase in the unsubstituted UAs (Fig. 1, panel a) despite a trace of it might be present in the vicinity of the triple Fi-1**k**/AI-1**k**/P point as discussed in Ref. 16. The IC phase becomes apparent in the selenium-doped crystals and the region of its occurrence increases with x. For $UAs_{0.9}Se_{0.1}$ (Fig. 1, panel d) the magnetic field of 13 T is not sufficient to destroy the incommensurate phase, whereas in $UAs_{0.97}Se_{0.03}$ (Fig. 1, panel b) and $UAs_{0.95}Se_{0.05}$ (Fig. 1, panel c) the IC phase survives only up to about $B \approx 2$ T and 6 T, respectively. Despite the fact that our thermodynamic data cannot unambiguously reveal an explicit type of magnetic order, we were capable to detect a mixed Fi-1**k**+Fi-2**k** state visible in Fig. 1 (panels b and c). We suppose that the region in the B-T phase diagram of $UAs_{0.9}Se_{0.1}$ (Fig. 1, panel d) denoted by the question mark can be a narrow stripe of the Fi-1**k** phase.

Figure 2 shows the magnified region of the phase diagrams in question for $x=0.03$ (panel a) and 0.05 (panel b) where the paramagnetic, incommensurate, and ferrimagnetic phases meet. The coordinates of these triple points along with coordinates of other specific points are given in Table I.

The nature of the converging phases at the Fi-1**k**/IC/P triple point suggests that this could be a case of a special multicritical point. Namely, it could be the Lifshitz point, at which commensurate and incommensurate phases are in equilibrium with the paramagnetic phase.[17] This possibility has been already discussed for the case of pure UAs, where neutron studies revealed diffuse critical scattering above T_N with the wave vector $k=0.7$ at $B=0$ T.[10,11] However, the particular type of phases (disordered, modulated, and ordered) that converge at the triple point it is not the only condition, which has to be satisfied to develop the canonical LP. In addition, the modulation wave vector of an incommensurate phase is expected to reach zero in the limit of the triple point. Although, in the case of $UAs_{0.97}Se_{0.03}$ (Ref. 3) and $UAs_{0.95}Se_{0.05}$ (Ref. 18) the neutron-diffraction studies showed that the wave vector in the absence of the magnetic field does not approach zero, when the temperature is nearing the P/IC transition. Specifically, slightly below T_N ($B=0$ T) $k=0.642$ for $x=0.03$, and $k=0.619$ for $x=0.05$.[5] Such a behavior of the wave vector does not fit into the framework of the theory proposed by Hornreich *et al.*[17] On the other hand, a similar phenomenon was already discussed by Qiu *et al.*[19] for sodium nitrate ($NaNO_2$) crystals, the properties of which were studied in transverse electric fields. The authors of Ref. 19 conclude that the Lifshitz point in systems

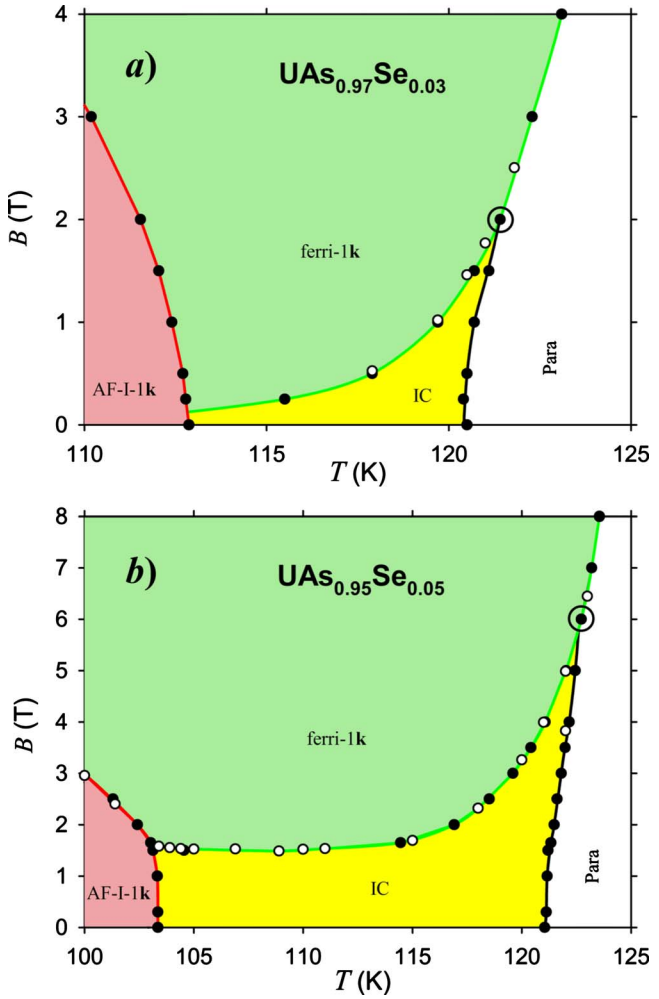

FIG. 2. (Color online) The B-T phase diagram of $UAs_{0.97}Se_{0.03}$ (upper panel a) and $UAs_{0.95}Se_{0.05}$ (bottom panel b) in the vicinity of the hypothetical Lifshitz point (indicated by open circles). Data points were obtained from specific-heat (solid points) and magnetocaloric (open points) measurements.

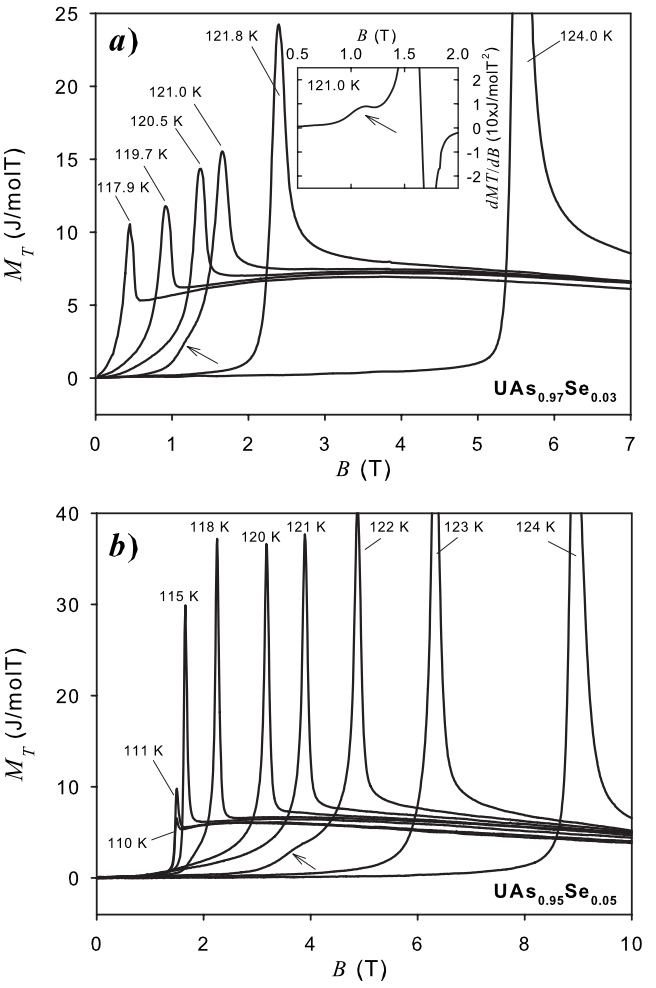

FIG. 3. The isothermal magnetocaloric coefficient curves when crossing the Fi-1**k**/IC and Fi-1**k**/P first-order phase transition lines for $UAs_{0.97}Se_{0.03}$ (upper panel a) and $UAs_{0.95}Se_{0.05}$ (bottom panel b). The data taken at $T=121.0$ K for $UAs_{0.97}Se_{0.03}$ and $T=122.0$ K for $UAs_{0.95}Se_{0.05}$ cross also the second order IC/P phase transition line (see Figs. 2 and 7) which is visible as a small bump indicated with an arrow. The inset in panel a shows an appearance of this anomaly (for $UAs_{0.97}Se_{0.03}$) in the derivative of the magnetocaloric coefficient with respect to the magnetic field. All curves were taken upon decreasing magnetic field.

which exhibit a discontinuous transition between disordered and ordered phases is physically inaccessible. Instead, they introduced an extension of the LP concept to first-order transitions. We believe that the case of $UAs_{1-x}Se_x$ may be similar since we see some evidence that the direct Fi-1**k**/P transition is of first order. The first hint comes from magnetocaloric data shown in Fig. 3. There is a peak at the transition in the field dependence of the magnetocaloric coefficient (B_{tr} and T_{tr} are coordinates of a given point on the Fi-1**k**/P transition line), which indicates that the phase transition involves latent heat. Furthermore there is no significant difference in the shape of the anomaly in $M_T(B)$ between the Fi-1**k**/IC (discontinuous) and the Fi-1**k**/P transitions. The anomalies in the specific heat at the IC/P and Fi-1**k**/P transitions as seen in Fig. 4 are evidently dissimilar. The first has a steplike shape that indicates a continuous phase transition, whereas the second is a peak. If the Fi-1**k**/P transition were of first order, it should obey a magnetic version of the Clausius-Clapeyron law

TABLE I. Coordinates of characteristic points on the B-T phase diagram of $UAs_{0.97}Se_{0.03}$ and $UAs_{0.95}Se_{0.05}$.

Compound	Characteristic point	T (K)	B (T)
$UAs_{0.97}Se_{0.03}$	Triple point (Fi-1**k**/AFI-1**k**/IC)	112.8	1.24
	Triple point (Fi-1**k**/IC/P)	121.4	~2
	Zero-field IC/P transition	120.5	0
	Zero-field AFI-1**k**/IC transition	112.9	0
$UAs_{0.95}Se_{0.05}$	Triple point (Fi-1**k**/AFI-1**k**/IC)	103.0	1.61
	Triple point (Fi-1**k**/IC/P)	122.6	~6
	Zero-field IC/P transition	103.4	0
	Zero-field AFI-1**k**/IC transition	121.0	0

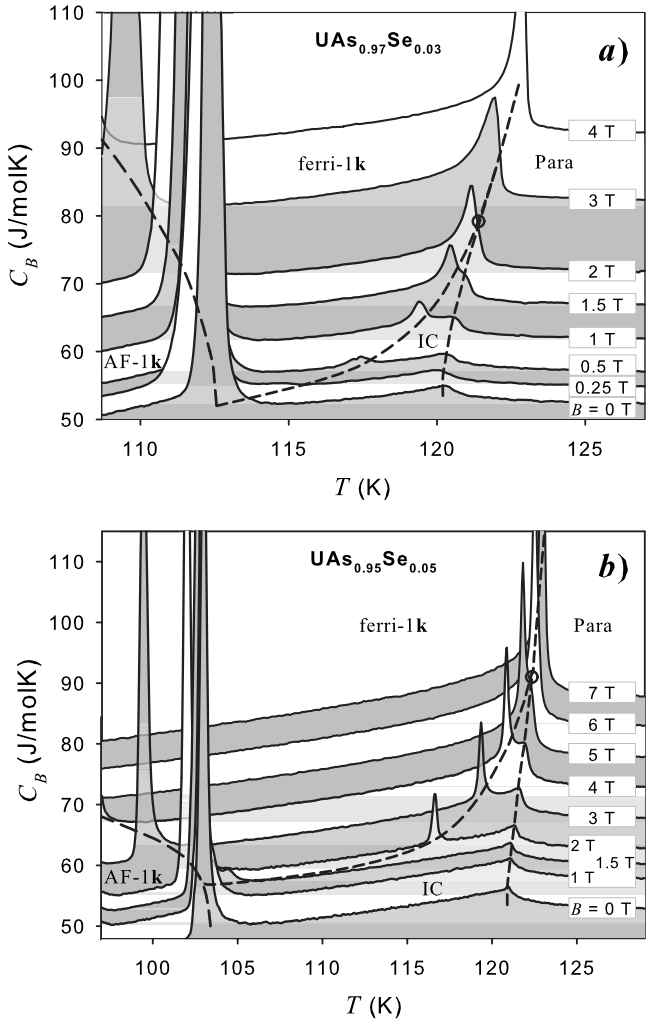

FIG. 4. The in-field specific heat of single-crystalline $UAs_{0.97}Se_{0.03}$ (upper panel a) and $UAs_{0.95}Se_{0.05}$ (bottom panel b). The respective values of the applied field are given in the small frames on the right side of the plots. Dashed lines denote the transition lines, which meet at the hypothetical LP denoted by an open circle. All curves were taken upon cooling.

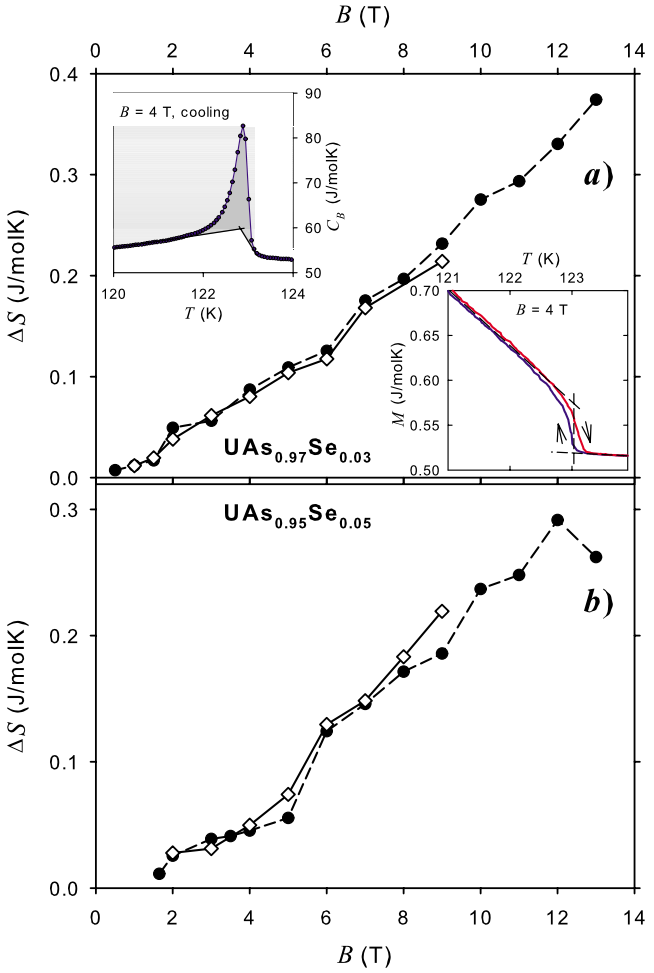

FIG. 5. (Color online) A comparison between the entropy jumps (ΔS) at the IC/P and Fi-1**k**/P transitions for $UAs_{0.97}Se_{0.03}$ (upper panel a) and $UAs_{0.95}Se_{0.05}$ (bottom panel b) calculated by two independent methods (see text for details): (1) full points refer to ΔS determined from the area of the peak from $C_B(T)$ data. The latent heat construction is shown in the upper inset in panel a. (2) Hollow diamonds refer to ΔS determined from the Clausius-Clapeyron equation. A jump in the molar magnetization is shown in the bottom inset to panel a.

$$\frac{dB_{tr}}{dT} = -\frac{\Delta S}{\Delta M}, \tag{1}$$

where dB_{tr}/dT is the slope of the phase transition line, ΔS is the entropy jump, and ΔM is the jump in the molar magnetization at the transition. ΔS can be independently obtained from either magnetocaloric or specific-heat measurements as

$$\Delta S = \frac{L}{T_{tr}}, \tag{2}$$

where L is the latent heat which is given by the integral of the total area between the peak and the baseline. We would like to emphasize that in the heat-flux method employed here the shape of a first-order anomaly is affected by the choice of measurement conditions (including a rate of the temperature/field sweep).[13] As a result, we usually observe at the first-order phase transition a linear ramp of $C_B(T)$, or $M_T(B)$, followed by an exponential relaxation, instead of a δ-functionlike shape. Nevertheless, an important fact is that the area between the peak and base line, and thus the estimated latent heat, remains independent irrespective of conditions.[13] In the studied case, different slopes of $C_B(T)$ above and below the transition make it impossible to find a proper single baseline. Therefore, the area of the peak was estimated under the assumption that at the transition we have a mixture of low- and high-temperature phases and their ratio changes with absorbed or released heat. An example of such a construction is shown in the upper inset of Fig. 5. The main panels of Fig. 5 present a comparison between the values of the entropy jump at the transition calculated independently by two different methods. The first method relies on using the Clausius-Clapeyron equation (1), where the $dB_{tr}(T)/dT$ slope and magnetization jump are experimentally deter-

mined. An example of estimation of ΔM is shown in the lower inset in Fig. 5). The second methods involves using the latent heat and Eq. (2). Both methods yield very similar values as expected for a first-order phase transition. In both samples ΔS is also found to be approximately proportional to the magnetic field. The IC/P, Fi/IC, and Fi/P phase transitions are easily visible in the specific heat and magnetocaloric data (see Figs. 3 and 4), although it is not straightforward to use these results for a precise evaluation of T_{tr} or B_{tr}. Both $C_B(T)$ and $M_T(B)$ dependences are measured by means of the dynamical method, thus shapes of first-order anomalies can be affected by rate of the temperature/field ramp as mentioned before. Therefore, we also performed measurements of the magnetic moment (M) and ac magnetic susceptibility (M') at a very low-temperature drift rate (0.05 K/min, $f=1011$ Hz, $B_{ac}=1$ mT). These results are presented in Fig. 6. The anomalies related to the phase transitions are much less obvious in $M(T)$ and $M'(T)$ than they were in the $C_B(T)$ data. However, we noticed that the transition temperatures correlate with sharp minima in the temperature derivative of the susceptibility. This allowed us to precisely determine $T_{\mathrm{Fi/IC}}(B)$, $T_{\mathrm{IC/P}}(B)$, and $T_{\mathrm{Fi/P}}(B)$ even in the region where the transition lines lie very close to each other. These results are shown in Fig. 7. From the analysis of the phase diagram of magnetic systems near LPs we know that $T_{\mathrm{Fi/P}}(B)$ and $T_{\mathrm{IC/P}}(B)$ lines should always be tangent whereas the $T_{\mathrm{Fi/IC}}(B)$ line is tangent to the other two only when the ordered phase is either uniaxial or easy plane with strong tetragonal anisotropy.[20] The phase diagram based on specific heat and magnetocaloric data (see Fig. 2) suggests that at least for $UAs_{0.95}Se_{0.05}$ the $T_{\mathrm{Fi/P}}(B)$ and $T_{\mathrm{IC/P}}(B)$ lines are nontangent. This finding seems to be proved independently by data shown in Fig. 7. This is further proof that we are not observing a canonical LP. Moreover, the nontangent order-disorder transition lines were anticipated by Qiu *et al.*[19] in the framework of their extended Lifshitz point concept.

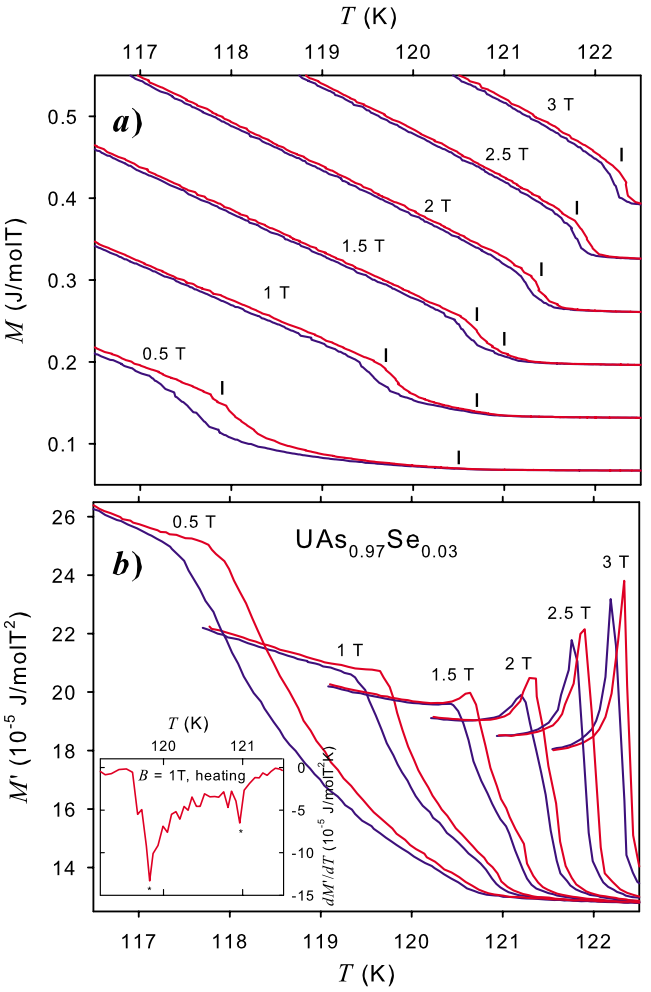

FIG. 6. (Color online) The temperature dependences of the magnetic moment [$M(T)$—upper panel a] and magnetic susceptibility [$M'(T)$—bottom panel b] of $UAs_{0.97}Se_{0.03}$. The "**I**" symbols indicate the transition temperatures as detected by calorimetric measurements. Red lines (to the right of the transition jumps) represent data taken upon warming while blue lines (to the left of the transition jumps) represent data taken upon cooling. The inset in panel b shows an example of a dM'/dT derivative plot, where minima indicated by asterisks are associated with the transition temperatures.

IV. LANDAU FREE ENERGY

The phase diagram even of pure UAs where only commensurate phases are observed is extremely complicated, showing an interplay between single- and double-**k** structures. It would be very difficult to propose and analyze a reasonable model which would describe the entire B-T phase diagram of this compound. Hence, we will confine our discussion to the paramagnet to ordered phase transitions as mentioned previously. These high temperature phase transitions from paramagnetic to the AI or ferrimagnetic phase in the presence of a magnetic field may be described by the phenomenological Landau free energy in the following form:

$$f_L = f_0 + v_1 m + v_2 m^2 + v_3 m^3 + a_f \phi_f^2 + c_f \phi_f^3 + b_f \phi_f^4 + a_a \phi_a^2 + b_a \phi_a^4 + d_f m \phi_f + d_a m \phi_a + d \phi_f^2 \phi_a^2, \quad (3)$$

where $v_1, v_2, v_3, a_f, b_f, c_f, a_a, b_a, d, d_f, d_a$ are temperature- and field-dependent coefficients. The variable m denotes a projection of the magnetization on the field direction, ϕ_f the ferrimagnetic, and ϕ_a the antiferromagnetic order parameters, respectively. A finite applied magnetic field leads to $m \neq 0$ and the free energy in Eq. (3) describes four types of states: the paramagnetic with $\phi_f=0$, $\phi_a=0$, and $m=m_P$

$$m_P = \frac{\sqrt{v_2^2 - 3v_1 v_2} - v_2}{3v_3} \quad (4)$$

and three ordered states: (i) the antiferromagnetic state with $\phi_f=0$

$$\phi_a = \sqrt{-\frac{a_a + d_a m}{2b_a}} \quad (5)$$

and

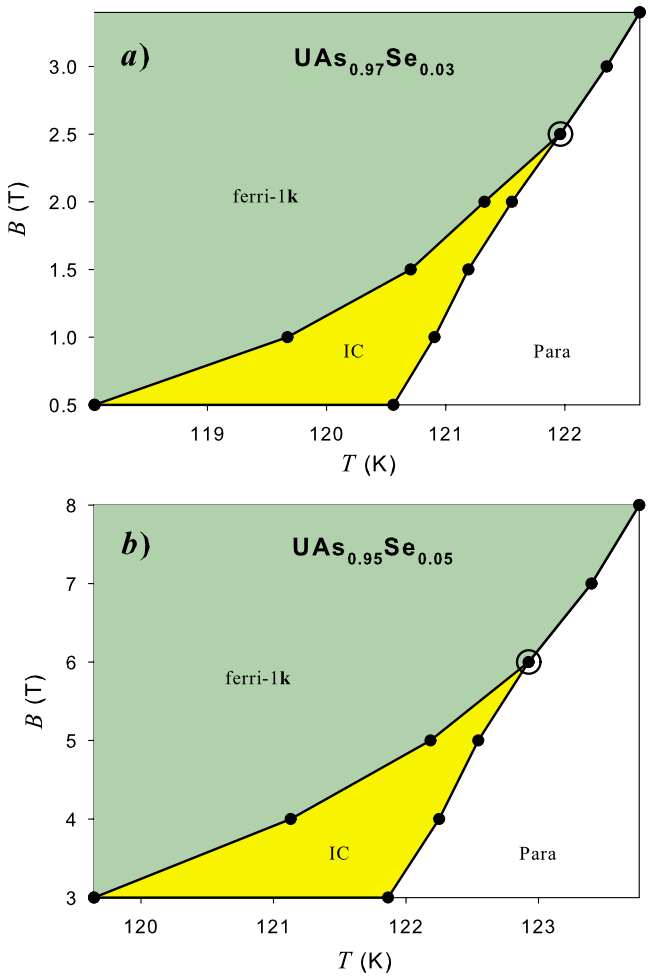

FIG. 7. (Color online) The B-T phase diagram of $UAs_{0.97}Se_{0.03}$ (upper panel a) and $UAs_{0.95}Se_{0.05}$ (bottom panel b) in the vicinity of the Fi-1**k**/IC/P triple point (indicated by open circles) as determined from the magnetic measurements (see Fig. 6 and the accompanying text for details).

$$m = \frac{\sqrt{d_a^2 - 4b_a v_2)^2 + 24b_a(a_a d_a - 2b_a v_1)v_3} + d_a^2 - 4b_a v_2}{12b_a v_3}, \tag{6}$$

(ii) the ferrimagnetic state with $\phi_a = 0$ and

$$\phi_f = \frac{1}{8b_f}\sqrt{-32a_f b_f + 9c_f^2 - 32b_f d_f m - 3c_f}, \tag{7}$$

where m is one of the solutions of the equation

$$3m^2 v_3 + 2mv_2 + \frac{d_f}{64b_f^2}(\sqrt{-32a_f b_f + 9c_f^2 - 32b_f d_f m} - 3c_f^2)^2 = 0, \tag{8}$$

and (iii) a mixed phase with $\phi_f = \phi_{fu} \neq 0$ and $\phi_a = \phi_{au} \neq 0$.

Unfortunately, a theory with a dozen or so free parameters [11 coefficients of the free energy in Eq. (3) and critical temperatures T_{ci}] is rather useless to describe the experimental data. To reduce this number of parameters one can try to reconstruct the Landau energy from some microscopic model. Kuznietz *et al.*[18] claimed that the magnetic behavior of the uranium monopnictides including UAs and solid solution $UAs_{1-x}Se_x$ is well accounted for by the so-called anisotropic-next-nearest-neighbor interaction model (ANNNI).[21] However, it seems that such a model is not sufficient enough even to describe the features of the high-temperature part of the UAs phase diagram. As seen from Fig. 1, an appropriate model should describe the phase transition from paramagnetic to the antiferromagnetic type-I phase for $B < B_p$ and for $B > B_p$ the phase transition to the ferrimagnetic phase, where both of the transitions are of first order. Let us consider the ferromagnetic layers with interlayer interaction j coupled by an extended ANNNI model in a magnetic field

$$\mathcal{H} = -j\sum_{i,j,n} S_i^n S_j^n - j_1 \sum_{i,j,n} S_i^n S_i^{n+1} - j_2 \sum_{i,j,n} S_i^n S_i^{n+2} - k_1 \sum_{i,j,n} S_i^n S_j^n S_i^{n+1} S_j^{n+1} - k_2 \sum_{i,j,n} S_i^n S_j^n S_i^{n+2} S_j^{n+2} - H\sum_{i,n} S_i^n, \tag{9}$$

where S_i^n denotes an Ising spin ($S = \pm 1$) in the "nth" layer and $H \equiv B/\mu$. In the Hamiltonian (9) the standard ANNNI model with the two-spin interactions (j, j_1, and j_2) is extended by taking into account the four-spin interactions (k_1, k_2). One should consider at least six layers to describe the high-temperature phase transitions to the AI phase with layers stacked in the (+−+−+−) sequence and the ferrimagnetic phase with layers (++−++−) phases. Let us denote the magnetization of the nth layer by $m_n = \langle S_i^n \rangle$ and introduce variables

$$m = \frac{1}{6}\sum_{n=1}^{6} m_n, \quad \phi_2 = m_1 + m_2 + m_3 - m_4 - m_5 - m_6,$$

$$\phi_3 = m_1 - m_3 \quad \phi_4 = m_2 - m_6 \quad \phi_5 = m_1 - m_4 \quad \phi_6 = m_3 - m_6. \tag{10}$$

Then the order parameters of the Landau free energy can be defined as

$$\phi_a = \phi_5 = \phi_6, \quad \phi_f = \phi_3 = \phi_4. \tag{11}$$

It is now easy to find all coefficients of the Landau free energy as functions of the microscopic parameters j, j_1, j_2, k_1, k_2, temperature T, and magnetic field H in the framework of the molecular field approximation

$$f_0 = -t \lg 2 \cosh\frac{H}{2t}, \quad v_1 = -2J \tanh\frac{H}{2t} \tag{12}$$

and

$$a_f = \frac{W\left(t - W + t\cosh\frac{H}{t}\right)}{9T\cosh^2\frac{H}{2t}}, \quad a_a = \frac{R\left(t - 2R + t\cosh\frac{H}{t}\right)}{4t\cosh^2\frac{H}{2t}}, \tag{13}$$

where $J=j+j_1+j_2$, $R=j-j_1+j_2$, $W=2j-j_1-j_2$, and $t=T/j$. It should be emphasized that the third-order term in the ferrimagnetic order parameter ϕ_f does not vanish in the Landau expansion in Eq. (3) and yields

$$c_f = -\frac{\tanh\frac{H}{2t}}{81t^2\cosh^2\frac{H}{2t}}\left[2W^3 + 3t^2K\left(1+\cosh\frac{H}{t}\right)\right]. \tag{14}$$

The other coefficients are given as

$$b_f = \frac{9Kt^3 - 12Kt^2W + 4W^4 + 2[6Kt^2(t-W) - W^4]\cosh\frac{h}{t} + 3Kt^3\cosh\frac{2H}{t}}{324t^3\cosh^4\frac{H}{2t}}, \tag{15}$$

$$b_a = \frac{32R^4 - 24KRt^2 + 9Kt^3 - 4(4R^4 + 6KRt^2 - 3Kt^3)\cosh\frac{H}{t} + 3Kt^3\cosh\frac{H}{t}}{192t^3\cosh^4\frac{H}{2t}}, \tag{16}$$

$$v_2 = \frac{J\left(t - J + t\cosh\frac{H}{t}\right)}{t\cosh^2\frac{H}{2t}}, \quad v_3 = \frac{\tanh\frac{H}{2t}}{3t^2\cosh^2\frac{H}{2t}}\left[8J^3 - 3Kt^2\left(1-\cosh\frac{H}{t}\right)\right], \tag{17}$$

$$d_f = \frac{4W^2J\tanh\frac{H}{2t}}{9t^2\cosh^2\frac{H}{2t}}, \quad d_a = \frac{8JR^2 + Pt^2\left(1+\cosh\frac{H}{t}\right)\tanh\frac{H}{2t}}{4t^2\cosh^2\frac{H}{2t}}, \tag{18}$$

where $K=k_1+k_2$ and $P=k_1-3k_2$. Now the number of the fitting parameters is reduced to four. Namely, j_1, j_2, k_1, and k_2 (one can assume $j=1$). However, this number is still too large in order to systematically present solutions of the model described by Eq. (3). Therefore, as an example we show the results for a model denoted as "A" which is defined by: $j_1=0.2$, $j_2=-0.71$, $k_1=-1.8$, and $k_2=-1$ (left plot in Fig. 8).

The phase transition lines from the disordered to type-AI and to ferrimagnetic phases merge at the multicritical point (H_p,t_p) denoted in Fig. 8 by open circles. For model A this point is located at (0.055,1.254). Figure 9 shows the ferrimagnetic order parameters and layer magnetizations for model A. In the ferrimagnetic phase the sequence of layers with magnetization $(m_1,m_1,m_3,m_1,m_1,m_3)$ is formed.

It is true that the simplest mean field approximation (MFA) fails to define the character of the phase-transition singularities and to quantitatively describe the thermodynamic properties of the system. However, it should predict a possibility of occurrence of several different phases. Let us start with the zero field case. The para-antiferromagnetic phase transition occurs at

$$a_a = \frac{R(t-R)}{2t} = 0. \tag{19}$$

Hence, at the transition point $(t=R)$ the fourth-order coefficient of the Landau theory in Eq. (17) reads

$$b_a = \frac{R^4}{12t^3} - \frac{K(2R-t)}{8t} = \frac{R}{3} - \frac{K}{2}. \tag{20}$$

According to the Landau theory the first-order phase transition, observed in UAs, occurs for $b_a<0$. The condition for such a transition is $K>\frac{2}{3}R$ from Eq. (20). Thus, K has to be finite and positive, which means that within the Landau theory the original ANNNI model cannot be used to describe the antiferromagnetic phase transition in UAs. To stabilize the antiferromagnetic phase for $b_a<0$ one should take into account the sixth order term (ϕ_a^6) in the Landau expansion. However, in this case, the solutions for the order parameter

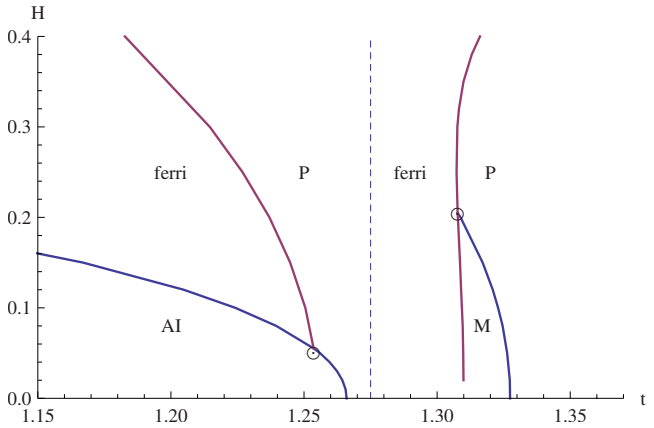

FIG. 8. (Color online) The (H,t) phase diagram of model A ($j_1=0.2$, $j_2=-0.71$, $k_1=-1.8$, $k_2=-1$)—left plot and B ($j_1=0.05$, $j_2=-0.67$, $k_1=-1.3$, $k_2=2.5$)—right plot. Open circles denote the multicritical points (H_p,t_p) for the A and B models, respectively

cannot be found analytically in the presence of an external field. Of course one could find the appropriate solutions numerically, but the number of the tunning parameters j_1,j_2,k_1,k_2, and H,t is too large in order to do it in a reasonable way without adequate experimental data, which according to our knowledge are not available.

Doping of UAs with Se changes the interaction parameters and an incommensurate phase for $H<H_p$ and $T<T_N$ appears. The properties of the spatially modulated phase of an Ising model with competing nearest-neighbors and next-nearest-neighbors interactions were studied by Monte Carlo methods[22] and by MFA.[23] In the latter paper the authors estimated the temperature-induced fluctuations and showed that the mean-field picture will hold even near T_c. They constructed the phase diagram with infinite number of commensurate phases and stated that near T_c all commensurate phases are narrow and the system is indistinguishable from an incommensurate one. The model proposed in the present paper cannot describe a true incommensurate phase as we have confined ourselves to six layers. However, for some set of the interaction parameters a kind of modulated phase (M) defined by

$$m_{i+1} = m_i - \delta \tag{21}$$

can be realized. To describe such a phase, instead of ϕ_2, ϕ_3, and ϕ_4 in Eq. (10) we will introduce new variables

$$\phi_2 = -\frac{1}{6}\sum_{n=1}^{6}(-1)^n m_n, \quad \phi_3 = m_1 - m_2 - m_3 + m_4,$$

$$\phi_4 = m_2 - m_3 - m_4 + m_5 \tag{22}$$

and now the order parameters are

$$\phi_f = \phi_3 = \phi_4, \quad \phi_u = 3\delta = \phi_2 = \phi_5 = \phi_6. \tag{23}$$

The form of the free energy is the same as in the previous case in Eq. (3) with ϕ_a,a_a,b_a replaced by ϕ_u,a_u,b_u, where for example,

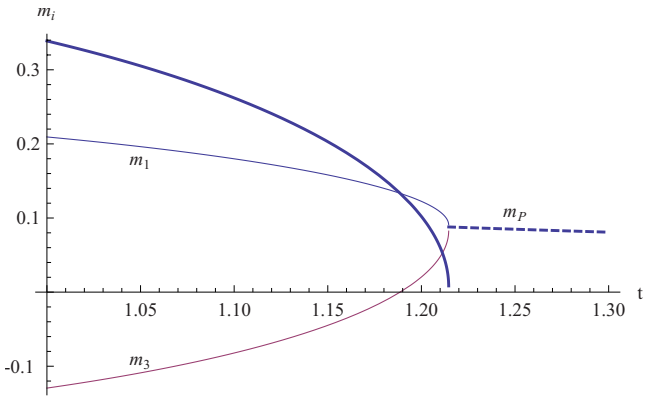

FIG. 9. (Color online) Model A: temperature dependence of the ferrimagnetic phase sublattice magnetization m_1 and m_3, bold line denotes the appropriate order parameter at $H=0.3$. The dashed line denotes the magnetization of the paramagnetic phase.

$$a_u = \frac{1}{108t\cosh^2\frac{H}{2t}}\left(-70j^2 - 22j_1^2 + 28j_1j_2 - 22j_2^2 + 5j_1t - 13j_2t + j(35t - 20j_1 + 52j_2) + (35j + 5j_1 - 13j_2)t\cosh\frac{H}{t}\right). \tag{24}$$

The appropriate phase diagram for a model denoted as "B" defined by ($j_1=0.05$, $j_2=-0.67$, $k_1=-1.3$, $k_2=2.5$) with three phases P, Fi, and M is presented in Fig. 8 (right plot) which can be compared with the high-temperature part of the phase diagram for $UAs_{0.97}Se_{0.03}$ from Fig. 2 (upper panel a). The second-order phase-transition line between paramagnetic and modulated phases meets the first-order transition line between paramagnetic and ferrimagnetic phases at the triple point ($H_p\approx 0.205$, $t_p\approx 1.308$). In fact, this multicritical point divides the first-order ferrimagnetic transition line into two segments, such that on the first the transition to the paramagnetic, while on the second to some modulated phase is observed. The first-order phase transition from simple ferromagnetic or antiferromagnetic to a modulated structure was predicted by Villain and Gordon.[24] It means, of course, that the multicritical (H_p,T_p) point cannot be considered as the canonical Lifshitz point which divides the second order transition line into two parts. In the M phase magnetization changes from layer to layer by δ which depends on the magnetic field and temperature. Figure 10 shows the temperature dependence of the layer magnetizations at $H=0.1$. In Fig. 11 the order parameters of the M and Fi phases are presented at $H=0.15$ (bold lines) and $H=0.2$ dashed lines. The modulated phase order parameter changes continuously while the ferrimagnetic exhibits a jump at the transition temperature.

To summarize this section, within the MFA the extended ANNNI model in Eq. (9) may be used to describe both high temperature triple points: (i) observed in undoped UAs where para-, ferri-, and antiferromagnetic phases meet and (ii) in selenium-doped crystals $UAs_{1-x}S_x$ for $x=0.03$ and 0.05 where the para-, ferri-, and modulated phases coexist. The parameter space of our model is quite rich (j_1,j_2,k_1,k_2)

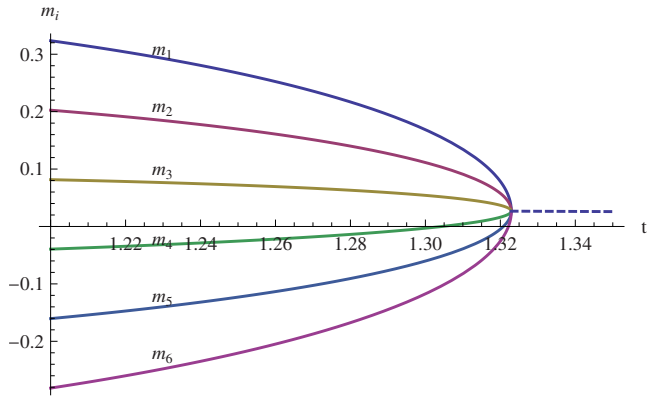

FIG. 10. (Color online) Model B: temperature dependence of the modulated phase layer magnetizations m_i at $H=0.1$. The dashed line denotes the magnetization of the paramagnetic phase.

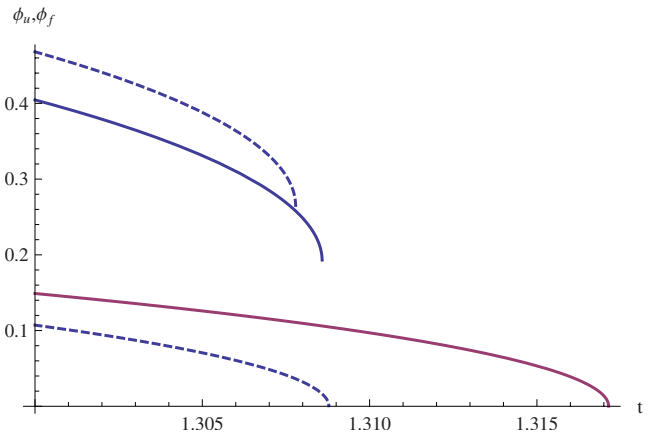

FIG. 11. (Color online) Model B: temperature dependence of the modulated (bottom curves) and ferrimagnetic (upper curves) phase order parameters at $H=0.15$ (bold lines) and $H=0.2$ (dashed lines).

and the values of these parameters can be fitted only based on experimental data which are not available as yet. Concerning the character of the phase transition, the results of the MFA may be not fully reliable and a more powerful approximation should be applied. However, we have found the values of the interaction parameters (model B) for which the P/M phase transition is continuous (second order) and Fi/P discontinuous (first order) (Fig. 11).

V. CONCLUSIONS

When introducing a new multicritical point Hornreich, Luban, and Shtrikman[17] suggested over 35 five years ago that "there exist a large number of systems in which a Lifshitz point may occur." Nevertheless, LP's have only been reported in a few systems to date. The authors of Ref. 17 mentioned $UAs_{1-x}S_x$ as the most promising system to find LP and there were suggestions that such a point may occur in similar $UAs_{1-x}Se_x$.[10] Our primary interest was therefore to check this possibility. To this end, we have systematically studied the magnetic phase diagram of $UAs_{1-x}Se_x$ single crystals for $x \leq 0.1$ in magnetic field up to 13 T. We report a yet unknown intermediate phase between Fi-1**k** and Fi-2**k** for $UAs_{0.97}Se_{0.03}$ and $UAs_{0.95}Se_{0.05}$ (see Fig. 1) which disappears for higher selenium content. We verified that doping UAs with Se stabilizes the modulated phase also in the presence of the magnetic field, and, in fact, the triple point, in which disordered (P), modulated (IC), and commensurate ordered (Fi) phases converge, is present in $UAs_{0.97}Se_{0.03}$ as well as in $UAs_{0.95}Se_{0.05}$. However, the critical behavior associated with this triple point is different from the canonical LP. Namely, in the studied case two transition lines are of first order and the boundary lines separating the ordered and disordered phases do not join with the same tangent. Thus, in view of Hornreich's[17] original idea regarding "a new multicritical point whose critical behavior is strikingly different from any reported previously" the extension of the LP concept to a first-order phase transition[19] has nothing to do with the main feature of LP i.e., critical behavior. Despite this, attempts are being made at labeling as LPs even those points in which all three incoming transition lines are of the first order,[25] i.e., where there is no critical behavior at all.

Further comprehensive experimental studies are also necessary for constraining the parameter values of the proposed extended ANNNI model. Nevertheless, this model, where the four-spin interactions in Eq. (9) are taken into account (on top of the ferromagnetic interactions j between each spin in the xy planes, the interactions between the spins in adjacent layers j_1, and the next-nearest layers j_2, as considered in the standard ANNNI model[22]) should be appropriate in describing main features of the high-temperature phase transitions in UAs and presumably in $UAs_{1-x}S_x$ as well.

ACKNOWLEDGMENTS

Authors would like to thank K. Mattenberger, O. Vogt, and G.H. Lander for significant contribution to this work and to L. J. Spalek for his comments. The research was supported by a Grant No. N N202 193234 of the Polish Ministry of Science and Higher Education.

[1] M. Obolenski and R. Troc, in *Proceedings of the Second International Conference on the Electronic Structure of the Actinides*, edited by J. Mulak, W. Suski, and R. Troc (Ossolineum, Wroclaw, 1977), p. 397.
[2] O. Vogt and H. Bartholin, J. Magn. Magn. Mater. **29**, 291 (1982).
[3] M. Kuznietz, P. Burlet, J. Rossat-Mignod, and O. Vogt, Solid State Commun. **55**, 1063 (1985).
[4] M. Kuznietz, P. Burlet, J. Rossat-Mignod, and O. Vogt, J. Less-Common Met. **121**, 217 (1986).
[5] M. Kuznietz, P. Burlet, and J. Rossat-Mignod, J. Magn. Magn. Mater. **69**, 12 (1987).

[6] M. J. Longfield, W. G. Stirling, E. Lidstrom, D. Mannix, G. H. Lander, A. Stunault, G. J. McIntyre, K. Mattenberger, and O. Vogt, Phys. Rev. B **63**, 134401 (2001).
[7] M. J. Longfield, W. G. Stirling, and G. H. Lander, Phys. Rev. B **63**, 134402 (2001).
[8] N. Bernhoeft, J. A. Paixao, C. Detlefs, S. B. Wilkins, P. Javorsky, E. Blackburn, and G. H. Lander, Phys. Rev. B **69**, 174415 (2004).
[9] B. Detlefs, S. B. Wilkins, P. Javorsky, E. Blackburn, and G. H. Lander, Phys. Rev. B **75**, 174403 (2007).
[10] S. K. Sinha, G. H. Lander, S. M. Shapiro, and O. Vogt, Phys. Rev. Lett. **45**, 1028 (1980).
[11] S. K. Sinha, G. H. Lander, S. M. Shapiro, and O. Vogt, Phys. Rev. B **23**, 4556 (1981).
[12] K. Mattenberger, L. Scherrer, and O. Vogt, J. Cryst. Growth **67**, 467 (1984).
[13] T. Plackowski, Y. Wang, and A. Junod, Rev. Sci. Instrum. **73**, 2755 (2002).
[14] J. M. Fournier and R. Troc, in *Handbook on the Physics and Chemistry of the Actinides*, edited by A. F. Freeman and G. H. Lander (North-Holland, Amsterdam, 1985), Vol. 2, pp. 29–173.
[15] J. Rossat-Mignod, P. Burlet, S. Quezel, O. Vogt, and H. Bartholin, in *Crystalline Electric Field Effects in f-Electron Magnetism*, Proceedings of the Fourth International Conference on Crystal-Field and Structural Effects in f-Electrons Systems, Wroclaw, Poland, 1981, edited by R. P. Guertin, W. Suski, and Z. Zolnierek (Plenum Press, New York, 1982), pp. 501–518.
[16] T. Plackowski, A. Junod, F. Bouquet, I. Sheikin, Y. Wang, A. Jezowski, and K. Mattenberger, Phys. Rev. B **67**, 184406 (2003).
[17] R. M. Hornreich, M. Luban, and S. Shtrikman, Phys. Rev. Lett. **35**, 1678 (1975).
[18] M. Kuznietz, P. Burlet, and J. Rossat-Mignod, J. Magn. Magn. Mater. **61**, 246 (1986).
[19] S. L. Qiu, Mitra Dutta, H. Z. Cummins, J. P. Wicksted, and S. M. Shapiro, Phys. Rev. B **34**, 7901 (1986).
[20] A. Michelson, Phys. Rev. B **16**, 577 (1977); **16**, 585 (1977); **16**, 5121 (1977).
[21] M. E. Fisher and W. Selke, Phys. Rev. Lett. **44**, 1502 (1980).
[22] W. Selke and M. E. Fisher, Phys. Rev. B **20**, 257 (1979).
[23] P. Bak and J. von Boehm, Phys. Rev. B **21**, 5297 (1980).
[24] J. Villain and M. B. Gordon, J. Phys. C **13**, 3117 (1980).
[25] I. Luk'yanchuk, A. Jorio, and P. Saint-Grégoire, Phys. Rev. B **61**, 3147 (2000).